Simulation of heat conductivity and charging processes in polar dielectrics induced by electron beam exposure

A Maslovskaya[1] and A Pavelchuk[1]

[1] Physics Engineering Department, Amur State University, 21, Ignatievskoe shosse, Blagoveshchensk, 675027, Russia
e-mail: maslovskayaag@mail.ru

Abstract. The article presents results of simulation of thermal and charging processes arising in polar dielectric materials analysed with scanning electron microscope techniques. Monte-Carlo simulation of electron transport in irradiated target was evaluated to realize field effect models. Simulation of thermal load and charging characteristics was performed using net-point methods. The analysis of injection, thermal and charging processes induced by electron irradiation in ferroelectrics subjected to experimental parameters are also discussed.

1. Introduction

Recently, one of the priority areas of condensed matter physics has focused on the problem of studying the basic laws and mechanisms of electron irradiation effects on dielectrics. This fact is due to wide applications of the analytical capabilities of scanning electron microscopy (SEM) for investigation and modification of various functional materials. Specific features of polar dielectrics and ferroelectrics, in particular, consist in sensitivity with respect to electrical and thermal exposure of the electron beam. This allows creating not only a potential contrast research methods, but also using an electron beam to study electrical properties of the samples as well as modify their polar structure. The electron beam injection activates the accumulation of absorbed electrons on the surface and in the bulk of sample, which, acting as an internal source, give rise to heating [1] and charging effects [2]. The previous studies based on experimental data has led to the point of view that effect of ferroelectric charging in the SEM has been considered as negative. To reduce the role of charging-up effects the low accelerating voltages (2-5 kV) have been employed [3]. However, the charging effect of ferroelectric material underlies a number of experimental techniques of direct polarization switching under electron beam exposure [4-6]. In addition the possibility of registration of the pyroelectric response due to thermal exposure of electron beam has been used to visualize ferroelectric domain structures with SEM pyroelectric mode [7].

Despite significant progress in the development of SEM experimental techniques the study of many effects is a difficult experimental problem. So in some cases, information on the behavior of the object can be obtained with the use of theoretical methods. The following main classes of models are usually considered to analyze the processes of electron beam interaction with solids. Firstly discrete stochastic models [8] based on Monte-Carlo method describe the electron transport in a sample. Secondly continuous-deterministic models enable field effects of injected charges [9-10] to be calculated.

However, information related to the specific study of polar dielectrics using different SEM modes as well as the study of corporate electron irradiation effects remains incomplete and requires further consideration. The present study was undertaken to simulate and analyze the dynamics of injection, thermal and charging processes occurring in the ferroelectrics irradiated by electron beam.

2. Simulation of field effects resulting from electron injection in irradiated polar dielectrics

2.1. Specification of electron injection process in irradiated sample

The first step both of thermal and charging processes simulation involves the estimation of initial electron distribution. The parameters of the electron irradiation doze and source function were estimated by a 3D-Monte-Carlo simulation of electron trajectories in the sample. We assumed that electrons with start beam energy E_0 fall perpendicularly to sample surface at point P_0. The electron position is defined by values of scattering angles: ω_i – azimuth angle and deviation angle – φ_i. The values of scattering angles and interaction mode are specified using random-number generator. An electron walks the distance s_i with energy E_i between stochastic scattering events:

$$s = -\lambda \ln(\xi), \quad \lambda = \frac{1}{N_0 \cdot \rho} \sum_{k=1}^{M} \frac{\omega_k \cdot A_k}{\sigma_k}, \tag{1}$$

where $\xi \in (0,1)$ is uniform distributed random quantity, λ is mean free path in m, A_k is atomic weight in g/mole, ω_k is weight fraction of element k, M is number of elements composing substance, σ_k is cross-section for each element k, in cm^2, N_0 is Avogadro's number in mole^{-1}, ρ is density in g/cm^3.

Mott cross-section was used to evaluate the total cross-section σ_k [11]. The computation of energy changes for inelastic electron scattering was based on modified form of Bethe law specified for multicomponent materials [8]:

$$\frac{dE}{ds} = -75800 \frac{\rho}{E} \cdot \sum_{k=1}^{M} \omega_k \frac{Z_k}{A_k} \ln\left(\frac{1.166(E + 0.8J_k)}{J_k}\right), \text{ keV/cm}, \quad Jk = \left[9.76Z_k + 58.5Z_k^{-0.19}\right] \cdot 10^{-3} \tag{2}$$

where Z_k is atomic number of element k, J_k is mean ionization potential of element k in keV.

The equation (2) for each electron position was solved numerically taking into account the initial condition specified as energy value at previous electron position. The changes in electron trajectories as well as energy loss were calculated for each electron till corresponding energy value decreases to threshold energy E_{th}~0.5 keV. According to Monte-Carlo method one needs performing simulation for rather significant electron histories N≈1000-10000 to achieve a statistical confidence.

2.2. Thermal process simulation of the electron beam interaction with ferroelectrics

In order to estimate the thermal effect of electron beam the some issuers should be considered: conditions of scanning modes, the geometry of model sample and internal source, thermalphysic characteristics of the object, conditions of experimental observation. The problem definition lies in the following. Focused electron beam has thermal effect on the sample. The geometry of model sample is shown in figure 1, where axis Z related to the symmetry axis of electron probe, the axes Y and X locate in sample surface plane. In addition «switching-on» of internal source occurs instantly in the sample and continuous heat source effects on the plane z=0 during the observation time.

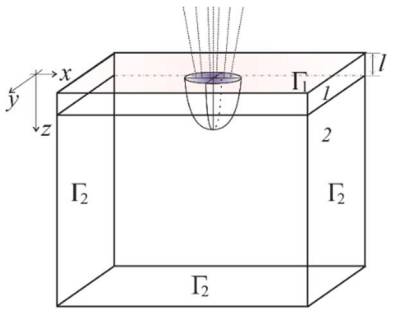

Figure 1. The geometry of model sample and approximation of internal heat source (for modes of high-voltage SEM).

The simulation can be performed for the sample covered by thin metal electrodes with thickness l. The half-spherical approximation of source was specified for the high-voltage SEM modes and the cylindrical approximation of the source was used for the low-voltage SEM modes. Contact resistance

is absent on the border surface. To approximate the internal source we employed Monte-Carlo simulation of electron trajectories in irradiated target.
The problem of nonstationary heat conductivity process simulation allows us to calculate the thermal distribution in polar material irradiated by focused electron beam particularly for the modes which use the thin metal electrodes covering the sample surface. The problem statement also includes initial, boundary conditions and conditions specified for metal-dielectric interface:

$$K_{xx}^i \frac{\partial^2 T_i}{\partial x^2} + K_{yy}^i \frac{\partial^2 T_i}{\partial y^2} + K_{zz}^i \frac{\partial^2 T_i}{\partial z^2} + f(x,y,z) = \rho_i c_i \frac{\partial T_i}{\partial t}, \quad T_i(x,y,t_0) = T_0,$$

$$T_i\big|_{\Gamma_2} = 0, \quad \left.\frac{\partial T_1(r,z,t)}{\partial z}\right|_{\Gamma_1} = 0, \quad i = \overline{1,2}, \quad k_1 \left.\frac{\partial T_1(M,t)}{\partial z}\right|_{z=l} = k_2 \left.\frac{\partial T_2(M,t)}{\partial z}\right|_{z=l}, \quad T_1\big|_{z=l} = T_2\big|_{z=l}, \qquad (3)$$

where T_i is temperature in K, K_{xx}^i, K_{yy}^i, K_{zz}^i are components of heat conductivity coefficient in W/(m·K), ρ_i is density in kg/m^3, c_i is specific heat capacity in J/(kg·K) in the layer *i, l* is thickness of metal electrode in m, $f=W/V$ is volume power density of heat source in W/m^3.
The general computational scheme for the problem (3) is based on combined net-point method, which permits expressing the temperature distribution on each temporal layer. Model (3) can be used for thermal load computation in the following practical cases: 1) for application of low-voltage as well as high-voltage SEM modes, 2) for experimental modes analyzing samples covered by thin metal electrodes, 3) for nonlinear temperature regime, 4) for object scanned by electron beam moving along one of the coordinate on the surface crystal, 5) for object scanned by pulsing electron probe.

2.3. Simulation of charging processes in polar dielectrics exposed to electron beam
In practice electric field potential is one of the constitutive quantity which characterizes charging effect in dielectrics. The classical general model describing dielectric charging process is based on combined solution of continuity equation and local-instantaneous Poisson equation:

$$\begin{cases} \dfrac{\partial \rho}{\partial t} = G - \operatorname{div} \mathbf{j} \\ \operatorname{div} \mathbf{E} = \dfrac{\rho}{\varepsilon \varepsilon_0} \end{cases} \qquad (4)$$

where ρ – charge density in C/m^3, $\mathbf{j} = \sigma\mathbf{E}$ is current density in A/m^2, σ – specific electric conduction in 1/(Ω·m), E is field intensity in V/m, ε is dielectric permittivity of sample, ε_0 is dielectric constant in C^2/(N ·m^2), G is generation component in C/(m^3·s).
Furthermore we used of relation between quantities which are associated with dimensions of distance and time: $\Delta t_{sc}=(\delta_{sc})^2/D$, where δ_{sc} is characterized by distance scale in m and D is defined as diffusion coefficient of electrons in m/s^2. This allows us to conclude that provided the irradiation occurs rather long time $t_{ir} >> \Delta t_{sc}$ then the stationary mode of charging process in some consideration is realized. The solving Poisson equation permits the potential distribution through crystal to be calculated depending on positions of injected charges. The problem statement of stationary charging process simulation is given by following form taking into account cylindrical symmetry of the problem:

$$\frac{\partial^2 \varphi}{\partial r^2} + \frac{1}{r}\frac{\partial \varphi}{\partial r} + \frac{\partial^2 \varphi}{\partial z^2} = -\frac{\rho(r,z)}{\varepsilon \varepsilon_0}, \quad \mathbf{E} = -\operatorname{grad} \varphi, \quad 0 \le r \le R, \quad 0 \le z \le Z. \qquad (5)$$

The boundary conditions are also specified to close the problem (5) as follows $\partial\varphi/\partial n = 0$ at r=0 and at z=0; $\varphi = 0$ at $r = R$ and at $z = Z$. Finite element method was used to calculate the potential as well as field intensity distribution created by volume charge distribution $\rho(r,z)$. In consideration of local character of charging process we also used modified computational scheme with minor size of elements covered injection area. Moreover the vector and absolute value of electron beam-induced polarization component can be estimated using the formula $\mathbf{P} = (\varepsilon - 1)\varepsilon_0 \mathbf{E}$.

3. Numerical experiment and result discussion

3.1. Estimation of electron beam injection characteristics

Figure 2 demonstrates the results of Monte-Carlo simulation of electron trajectories obtained for $LiNbO_3$ crystal. The analysis of computational results for typical ferroelectrics irradiated by electron beam with averages energies E_0=1-40 keV indicates that geometry of the area of electron beam interaction with samples can be characterized by semispherical or semi-ellipsoidal form (mostly for inorganic crystals such as $LiNbO_3$, $BaTiO_3$, $LiTaO_3$) and "pear-shaped" form (for organic type crystals such as TGS, DTGS, CH_4N_2S) depending on elemental composition.

The simulation results allow us to conclude that when start beam energy increases the form of the curve enveloping area of electron interaction with samples extends lengthwise coordinate axis *OZ*. Absolute value of electron injection depth does not depend on size of irradiated area on the sample surface. In addition the presence of metal electrode does not prevent electron injection into the sample and type of metal electrode (Ag, Au, Cu) results in approximately similar electron injection depth.

To initialize the internal source function let us consider function of electron density distribution, which can be specified using Gauss distribution for local irradiated area as follows:

$$I(r,z) = I_0 \cdot \exp\left(-\left(\sqrt{r^2+z^2}-\delta_1\right)^2 / \left(2\cdot(\delta_2)^2\right)\right), \quad r=\sqrt{x^2+y^2} \tag{6}$$

where I_0 is normalization constant; δ_1 and δ_2 are parameters numerically estimated by means of least square procedure.

The figure 3 illustrates computational result of the profile of normalized energy loss distribution obtained with use of equation (6).

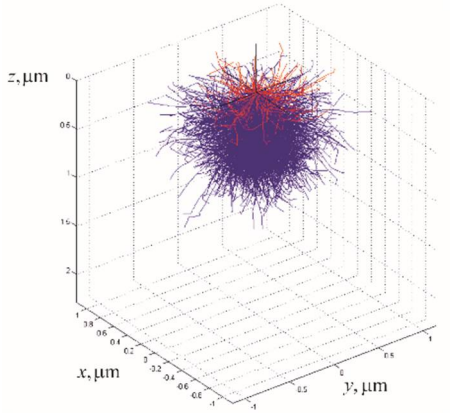

Figure 2. The result of Monte-Carlo simulation of the area of electron beam interaction with $LiNbO_3$ sample at start beam energy E_0=10 keV, beam diameter d=1 μm, N=10000 electron histories.

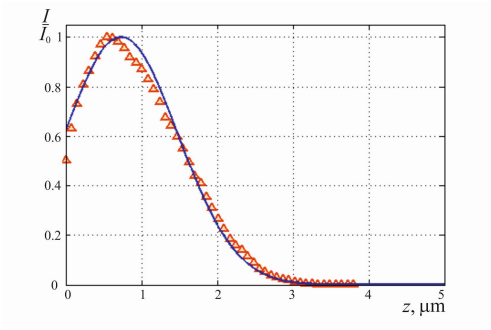

Figure 3. The approximation depth profile of electron energy loss distribution obtained by Monte-Carlo simulation of electron transport in $LiNbO_3$ at start beam energy E_0=25 keV, beam diameter d=2 μm, N=10000 electron histories.

3.2. Computation of electron beam-induced thermal loading effects in ferroelectrics

In order to perform simulation of temperature distributions the characteristic parameters need to be estimated. In general one should determine geometrical size of sample and electrode thickness, thermal characteristics of sample and electrode, the time of source action, initial temperature of the sample as well as accelerating voltages and probe current. The equation (6) is used to express volume power density of heat source taking into account the approximation of area of electron beam interaction with material and also the value of source power.

The simulation was performed taking into account various parameters of the samples and experimental conditions. Specifically uncoated sample surface as well as ferroelectric coated by with thin metal electrodes were considered. The curves in figures 4 and 5 demonstrate the calculated dynamic temperature profiles attributed to typical ferroelectric crystals.

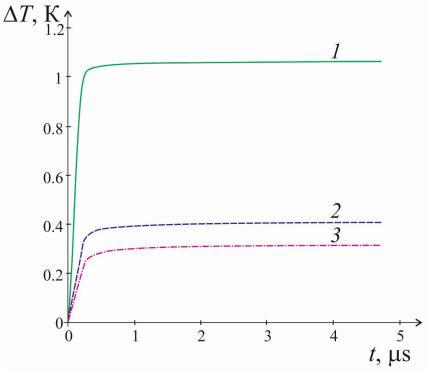

Figure 4. Dynamic dependence of overheat level $\Delta T=T-T_0$ ΔT for $LiNbO_3$ at electron beam position with energies: 1 – E_0=15 keV, 2 – E_0=25 keV, 3 – E_0=40 keV.

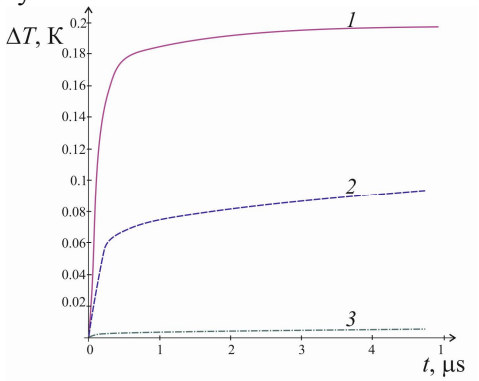

Figure 5. Temperature dynamics ΔT at electron beam position for $BaTiO_3$: 1 – observation on the uncoated sample, 2 – on the sample coated by silver electrode with thickness l=1 μm and 3 – l=10 μm.

The overheat level of typical ferroelectric crystals (TGS, DTGS, $LiNbO_3$, $LiTaO_3$, $BaTiO_3$, $NaNO_2$) in high-voltage SEM mode are estimated to be magnitudes of order of several Kelvins. These values can not cause heat damage of the samples although changing in temperature gradient can activate pyroelectric effect which impacts on videosignal. This aspect is essential point of ferroelectric domain structure observation with pyroelectric mode of SEM [7].

The figure 4 demonstrates plotted dynamic temperature profiles for $LiNbO_3$ at different values of accelerating voltages. The increasing in source power leads to decreasing in temperature. These results suggest that temperature gradient can affect videosignal and controlled heating level in SEM modes requires increasing source power due to increasing current of the probe. The figure 5 displays the plotted dynamic temperature profiles for $BaTiO_3$ depending on presence and thickness of metal electrode. According to the results the use of coated samples considerably reduces the thermal load. The use of modes with samples coated by metal electrode is essential for thermal estimations. The increasing of electrode thickness leads to decreasing of overheating level. Experimental methods (using thermocouple) result in rough results due to influence of thermocouple on temperature distribution in the sample volume. The latter has previously also been noted in [1].

3.3. Computing characteristics of charging process

The geometrical size of the sample, dielectric permittivity as well as initial charge distribution were determined to calculate following charging characteristics: potential, field intensity distribution and polarization component electron beam induced. The computation of ρ_0 requires initialization of accelerating voltages U, electron beam diameter d, surface density of injected charge σ_{surf} at given probe current I. The function $\rho_0(r,z)$ was defined using equation (6) based on Monte-Carlo simulation of electron trajectories in a sample. The figure 6 shows model potential distribution and depth profile of field intensity absolute value calculated for $LiNbO_3$. The magnitude of the field on the border of injection area is rather more than coercive field for $LiNbO_3$ ($2\cdot10^7$ V/m). The evidence from this study confirm that electron injection into the ferroelectric sample can result in charge accumulation. The field of accumulated charges is able to stimulate intensive repolarization processes in domains "tail-to-beam" orientated. This effect has been observed experimentally in [5]. The simulation results indicate that increase in start beam energy E_0 at fixed value of surface density of injected charges σ_{surf} leads to reducing levels of maximum values of φ, E and P due to increase in volume of internal source.

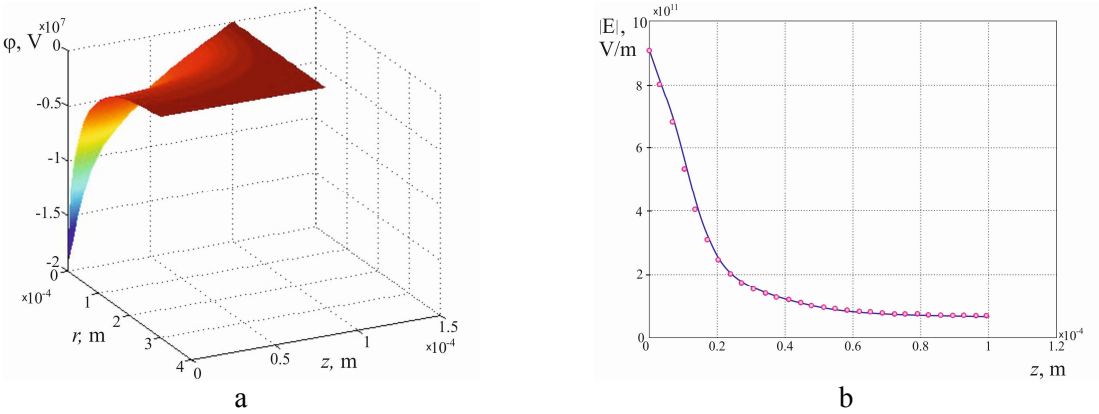

Figure 6. The simulation results of potential distribution – a, the depth profile of field intensity absolute value at point r=0 for $LiNbO_3$. The irradiation dose correspond to surface density of injected charges σ_{surf}=400 C/m^2 (irradiated area S=10^{-10} m^2, probe current I=200 pA), E_0=10 keV, d=14 μm.

Control of charging characteristic process needs to adjust the following parameters. The electron beam current I determines injected charge value ΔQ and therefore surface density of injected charges σ_{surf}. Moreover accelerating voltages U specify electron beam energy E_0 and volume of internal source ΔV.

4. Conclusion

Thus this study presents the simulation results of injection, thermal and charging processes of electron beam interaction with polar dielectrics. The description of geometrical form of electron beam interaction area was demonstrated using the Monte-Carlo simulation of electron transport. The criteria limiting the thickness of metal electrode were determined to analyze ferroelectrics with injective SEM modes. Also the thermal field simulation enables heat load of electron beam to be evaluated at various given SEM experimental parameters. The estimations of electrical characteristic due to charging effects at increased accelerating voltages indicate that controlled initial data of probe current as well as start beam energy can lead to arising significant field intensity values and as a consequence this can create conditions for domain structure reorientation under electron beam exposure.

Acknowledgments

The work has been supported by a scientific program of the Ministry of Education and Science of Russia (project No.1158.2014/9).

References

[1] Filippov M N 1993 *Izvestiya Akademii Nauk Seriya Fizicheskaya* **8** 163
[2] Cazaux J 1986 *J. Appl. Phys.* **59** 1418
[3] Le Bihan R 1989 *Ferroelectrics* **97** 19
[4] He J, Tang S H, Qin Y Q et al. 2003 *J. Appl. Phys.* **93** 9943
[5] Molina P, Ramírez M O, García-Sole J, Bausá L E 2009 *Optical Materials* **31** 1777.
[6] Maslovskaya A G, Kopylova I B 2009 *JETP* **108** 1144
[7] Latham R V 1976 *J. Phys. D: Appl. Phys.* **9** 2295
[8] Joy D C 1995 *Monte-Carlo modeling for electron microscopy and microanalysis* (New York: Oxford University Press)
[9] Bakaleinikov L A, Galaktionov E V, Tret'yakov V V, Tropp E A 2001 *Physics of the Solid State* **43** 779
[10] Suga H, Tadokoro H, Kotera M 1998 *Electron microscopy* **1** 177.
[11] Czyzewski Z, MacCallum D O, Roming A, Joy D C 1990 *J. Appl. Phys.* **68** 3066.